

Rechargeable Aqueous Microdroplet

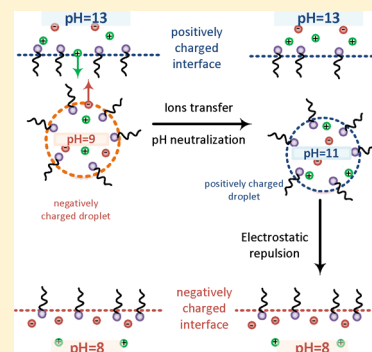
Chi M. Phan*

Department of Chemical Engineering, Curtin University, Perth, WA 6845, Australia

S Supporting Information

ABSTRACT: Directional and controllable transportation of microdroplets is critical for emerging micro- and nanotechnology, in which the conventional mechanical energy generation is not applicable. This Letter shows that an aqueous microdroplet can be charged for controlled motion in electrostatic potential, which was created by differentiating pH, between two oil/water interfaces. The directional motion of the droplet, <math><100\ \mu\text{m}</math> in diameter, was obtained with a constant velocity of $\sim 1\ \text{mm/s}$. The force analysis showed that the droplet surface was charged and recharged oppositely by ion transfer through interfacial layers, without significant mass transfer. The charging and recharging cycles were recorded continuously with a single droplet over 100 times. The energy for motion was generated from pH neutralization, which is the simplest aqueous reaction. This is the first time that the phenomenon is reported. The phenomenon can be employed as an efficient and robust method to convert chemical to mechanical energy for miniaturized devices and microprocesses.

SECTION: Surfaces, Interfaces, Porous Materials, and Catalysis



It has been well-accepted that a water interface with air, an immiscible liquid, or solid can have a non-neutral charge due to the presence of an electrical double layer.¹ Owing to experimental difficulties, the exact potential of an air/water surface remains elusive, with reported values varied from -1.1 to $0.5\ \text{V}$.^{2,3} Nevertheless, all studies agreed that the air/pure water surface charge is non-neutral. In practice, the interfacial potential is deterministically correlated to controllable factors in the aqueous phase, such as surfactants⁴ and ionic strength.⁵ More significantly, the interfacial potential of both solid/liquid⁶ and air/liquid interfaces⁷ can be switched from positive to negative by changing the pH of the aqueous phase. Therefore, the potential of the oil/water interface is expectedly tunable with pH.⁸ The maximum potential difference between two oil/water interfaces could be less than $0.5\ \text{V}$, which is insignificant for most macroprocesses. Yet, it should be sufficient to drive the liquid micro- and nanodroplets, if charged appropriately, over a submillimeter distance. This could provide an efficient and practical microtransportation method. The quest of such transportation has been pursued with great interest by using solid surface pattern,⁹ light,^{10,11} a thermal gradient,¹² magnetism,¹³ dielectrophoresis,¹⁴ an electrocapillary,¹⁵ or an external potential.¹⁶ The controlled transportation of microdroplets is critical for emerging micro- and nanotechnology, in which the conventional mechanical energy generation is not applicable. More recently, chemical reactions within the microdroplets^{17,18} have been promoted as an attractive alternative. However, there are some disadvantages of chemically self-propelled microdroplets. First, the droplet trajectory is not controllable. Second, the microdroplets have to be created with chemical “fuels” inside, for example, H_2O_2 , and cannot be “refueled”. Furthermore, the chemical reaction is controlled by catalysts, which can be quickly poisoned.¹⁹

This study used the setup in Figure 1; the top and bottom aqueous solutions acted as two reservoirs with different pHs and thus created an electrostatic potential between the two oil/water interfaces. For instance, the experimental setup was obtained with pHs of 8 and 13 in the bottom and top reservoirs, respectively. The two water/oil interfaces were separated by an oil layer, $\sim 1\ \text{mm}$. The top aqueous droplet was held by the oil/air and water/air interfacial tensions.²⁰

When a microdroplet was formed, it was attracted to one interface, became charged, and started bouncing between the two interfaces repeatedly (Figure 1 and Movie S1, SI). More than 200 cycles were observed with a single droplet. The observation resembled a reported bouncing phenomenon in which oppositely charged droplets attracted to and bounced away from each other without coalescing.²¹ The previous bouncing observation was contributed to the existence of a short-lived ($<80\ \mu\text{s}$) and narrow conductive bridge, through which the charge was transferred without significant mass transfer. Such bouncing was only obtainable in an external potential greater than $200\ \text{V/mm}$, below which the two liquid/liquid interfaces coalesced. In contrast, the electrical field in this study was generated by the interfacial potential, which should be less than $0.5\ \text{V/mm}$. The contacting times between the droplet and interfaces, that is, the charge-transfer periods, were more than $10\ \text{ms}$. The following force analysis demonstrated that the ion transfer was driven by interfacial phenomena, rather than the bulk transportation phenomena.

The trajectory of the droplet was recorded and analyzed as image sequences. The droplet was detected using the edge

Received: March 18, 2014

Accepted: April 4, 2014

Published: April 4, 2014

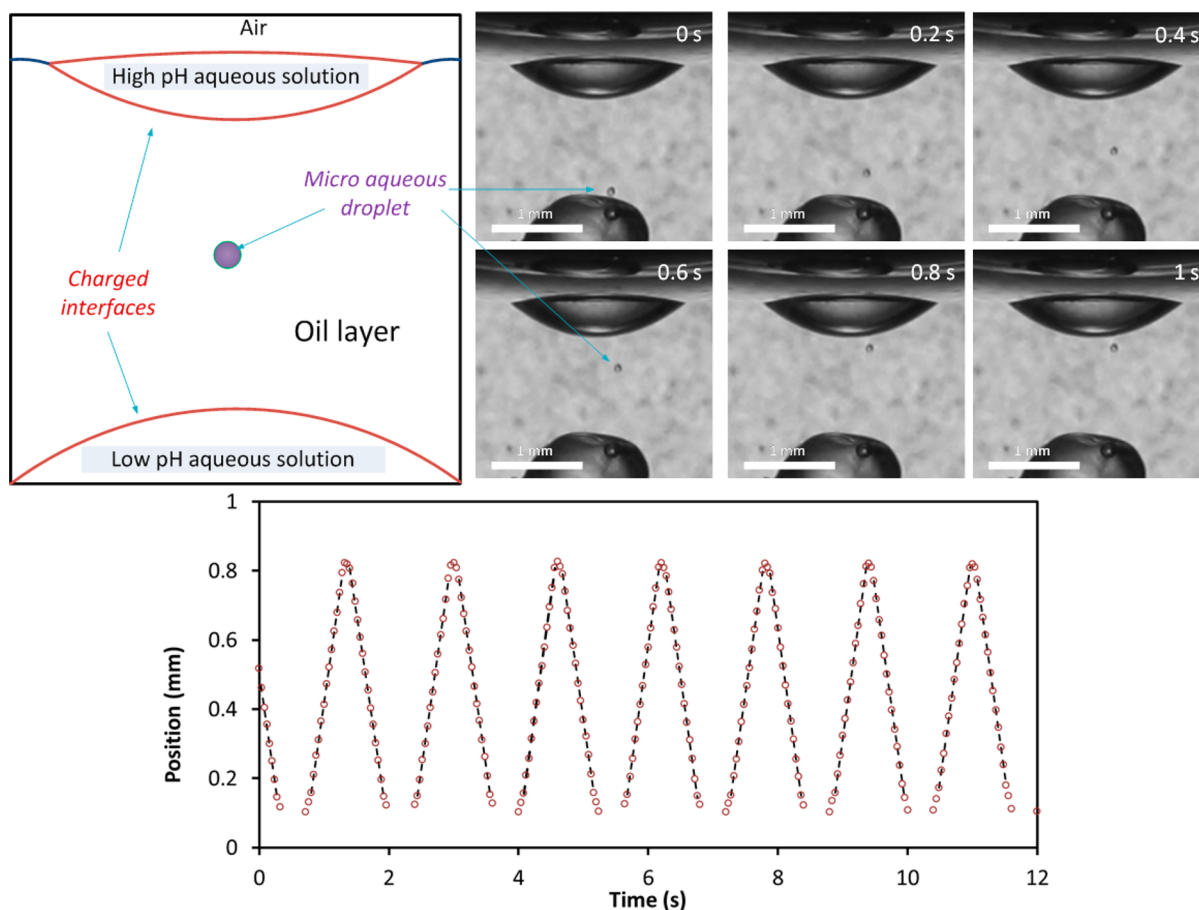


Figure 1. (Top) Experimental setup and raw images (a movie is supplied in the Supporting Information (SI)); the droplet diameter was $91 \mu\text{m}$. (Bottom) Droplet vertical position as a function of time (broken lines represent a linear regression).

detection function in MATLAB for each image. Consequently, the location of the droplet center was obtained and tracked as a function of time. It can be seen that the droplet reached the terminal (constant) velocity within 0.1 s after repulsion, as shown in the vertical position profile in Figure 1. In contrast, the other bouncing phenomenon was still in acceleration.²¹ From the terminal velocity, the drag force can be calculated and used to predict the driving forces, that is, electrostatic and gravity. It should be noted that the dielectric force is not included because the minimum threshold for a significant dielectric force within an aqueous droplet is $\sim 90 \text{ V/mm}$.²² Detailed calculations (in the SI) showed that the gravitational force was less than 3% of the total drag force for the droplet with a diameter of $91 \mu\text{m}$. Obviously, the force contribution can be controlled by varying physical properties, namely, densities, viscosity, and droplet size. Furthermore, the electrostatic force can be controlled by changing the separation distance between the two interfaces. An example of the slower motion is shown in Movie S2 (SI), in which the separating distance was 1.7 mm.

From the electrostatic force, the potential energy of the droplet can be easily calculated for each trip. At the beginning, the terminal velocities were almost the same for both upward and downward legs (Figure 2a), which indicated that the droplet surface was charged oppositely with a similar magnitude between the two legs of the cycles. Assuming a typical value of ΔV at 0.5 V, the charge of the droplet can be calculated from the electrostatic energy. Accordingly, the ionic concentration of the droplet surface, which is positive for the upward and

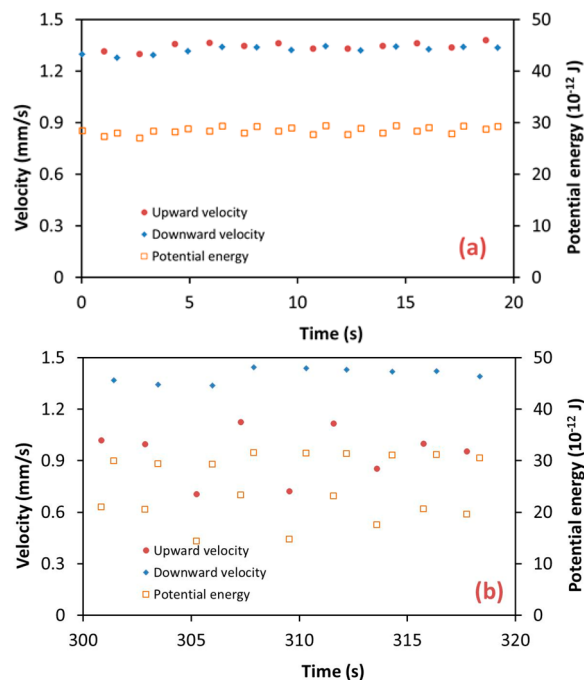


Figure 2. Droplet vertical velocity and force analysis (a) at the beginning and (b) after 5 min.

negative for the downward trip, was calculated to be $\sim 2.28 \pm 0.05 \times 10^{-8} \text{ mol/m}^2$. The obtained surface charges were of the

same order of magnitude for the charge at the air/aqueous alcohol interface, $\sim 10^{-8}$ mol/m².²³

Mechanism. The coalescence of the microdroplet with oil/water interfaces was prevented by a cohesive film at the oil/water interfaces and droplet surface. Such a cohesive film has been reported for the naturally occurring asphaltenes in the literature.²⁴ The film can be stabilized by high pH and multivalent cations,²⁵ which was Fe³⁺ in this case. A similar film was also reported with microgel, which prevented the coalescence between oppositely charged microdroplets.²⁶ However, the film in this study allowed effective charge transfer. Because the reservoirs were electrically isolated, the charge was transferred in the form of ions, such as H₃O⁺, OH⁻, Na⁺, Cl⁻, and so forth. During the contacting period, the ions were transferred through the oil film and eventually changed the pH inside of the droplet. For example, the proposed ion transfer at the top interface is shown in Figure 3. The surface

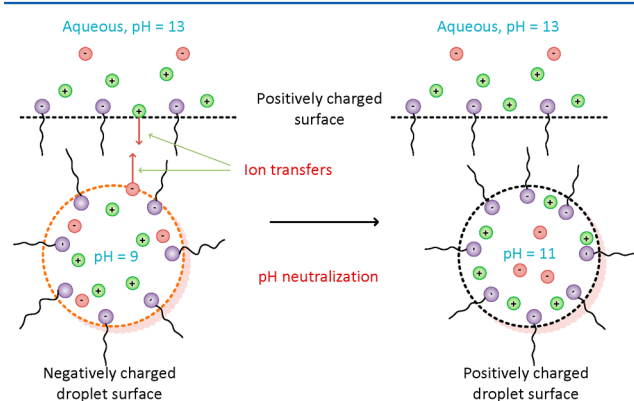


Figure 3. Proposed charge transfer during the contacting period at the top interface.

potential was expectedly changed from negative to positive with the increasing pH in a monotonic correlation. As a result, the droplet surface was charged with the same sign as the contacting interface and was repulsed from the interface. The energy of pH neutralization was transferred into the potential energy during the contacting period. After detaching, the potential energy was converted into kinetic energy and drove the droplet to the other side, similar to charged particles in an electrostatic field. At the bottom interface, the droplet was charged oppositely, namely, from positive to negative, by the low pH reservoir. The repeating cycles indicated that ion transfer involved both cations and anions, and the net ionic transfer was zero. In the motion with external potential,²¹ in contrast, the net ionic transfer was one-way only and directed by the external electrical current.

Although the exact pH inside of the droplet is not known, a moderate pH increment from 9 to 11 would give enough energy for the motion. It should be noted that the neutralization energy varies with the pH gradient as well (example calculations are included in the SI).

The reaction also happened within the two reservoirs and thus gradually changed pH in the two reservoirs. Consequently, the energy conversion was different from that of the two ends. The motion after 5 min, ~ 150 cycles, clearly highlighted the inefficiency of the ion transfer at a lower pH gradient (Figure 2b); the upward velocity was inconsistent and much lower than the downward velocity. The completion time for each cycle was also noticeably longer than that of the beginning cycles (Figure

2a). The reduction in velocity indicated a weaker electrostatic force, which can be attributed to (i) the reduced potential gradient and (ii) the reduced charge of the droplet. These collectively indicated that the kinetics of ion transfer and the recharging process depends on the pH of the solutions. At a lower pH gradient, the ion transfer becomes slower and less effective.

If one interface was not stabilized by the cohesive film (e.g., in strong acidic conditions), the droplet remained adhesive to and coalesced with the interface after contacting. In this case, a one-way trip was obtained.

In summary, the fuels for droplet motion in this phenomenon, cations and anions, were added after the droplet formation, and the droplet could be refueled indefinitely. This is a key advantage over the current chemical method,^{17,19} in which the microdroplet cannot be refueled after formation. The obtained velocity, ~ 15 body lengths per second, was comparable to other methods in the literature.²⁷ Furthermore, the velocity can be precisely controlled by changing the droplet size, the separating distance, or oil viscosity. The motion remained constant for a significant period, ~ 100 cycles, before slowing down. Afterward, the constant motion could be easily maintained by adding more base/acid into the respective reservoirs. A striking implication of the phenomena was that a microtaxi can be driven back and forth repeatedly. The mechanical energy of this transportation ultimately comes from the simplest aqueous reaction, pH neutralization. This presents an efficient method for controllable chemical machinery, namely, a tunable transduction of chemical energy into mechanical energy at the microscale.²⁸

In addition to controlling liquid motion in the microchannel,²⁹ the findings open new opportunities to design a water gate on the nanoscale³⁰ and nanodroplet manipulation.³¹ In the literature, the cohesive “film” at the oil/water interface has been reported with biosurfactants, such as peptides^{32,33} and lecithin.³⁴ Because the biological cell membranes and vesicles are formed in a similar manner, that is, surrounded by a lipid bilayer, one might expect to find the phenomena in vivo as well.

METHODS

Paraffin oil was obtained from Digger, Australia. The oil viscosity and density were 830 kg/m³ and 22 cP, respectively. Sodium dodecyl sulfate (SDS), FeCl₃, NaOH, HCl, and NaCl were obtained from Sigma-Aldrich. The aqueous solution was prepared with deionized water and contained 8 mM SDS, 1 wt % FeCl₃, and 3.5 wt % NaCl. The solution was divided into two portions for pH adjustment by adding either NaOH or HCl. The low-pH solution was deposited in a transparent container. Subsequently, a thin oil layer was deposited on top. The high-pH solution was used at the top reservoir, as a floating aqueous lens. At the beginning of the experiment, ~ 8 μ L of high-pH solution was deposited on the oil/air surface. The droplet formed a liquid bridge and broke into the satellite droplets, one of which was used as the microdroplet for the analysis. The motion was captured by a digital camera with a microscopic lens.

ASSOCIATED CONTENT

Supporting Information

Two movies are supplied, showing a microdroplets behavior with two interfaces. The force analysis is also included. This material is available free of charge via the Internet at <http://pubs.acs.org>.

■ AUTHOR INFORMATION

Corresponding Author

*E-mail: c.phan@curtin.edu.au.

Notes

The author declares no competing financial interest.

■ REFERENCES

- (1) Bazant, M. Z.; Squires, T. M. Induced-Charge Electrokinetic Phenomena: Theory and Microfluidic Applications. *Phys. Rev. Lett.* **2004**, *92*, 066101.
- (2) Kathmann, S. M.; Kuo, I. F. W.; Mundy, C. J. Electronic Effects on the Surface Potential at the Vapor–Liquid Interface of Water. *J. Am. Chem. Soc.* **2008**, *130*, 16556–16561.
- (3) Hanni-Ciunel, K.; Schelero, N.; von Klitzing, R. Negative Charges at the Air/Water Interface and their Consequences for Aqueous Wetting Films Containing Surfactants. *Faraday Discuss.* **2009**, *141*, 41–53.
- (4) Nakahara, H.; Shibata, O.; Moroi, Y. Examination of Surface Adsorption of Cetyltrimethylammonium Bromide and Sodium Dodecyl Sulfate. *J. Phys. Chem. B* **2011**, *115*, 9077–9086.
- (5) Phan, C. M.; Nakahara, H.; Shibata, O.; Moroi, Y.; Le, T. N.; Ang, H. M. Surface Potential of Methyl Isobutyl Carbinol Adsorption Layer at the Air/Water Interface. *J. Phys. Chem. B* **2012**, *116*, 980–986.
- (6) Brown, M. A.; Beloqui Redondo, A.; Sterrer, M.; Winter, B.; Pacchioni, G.; Abbas, Z.; van Bokhoven, J. A. Measure of Surface Potential at the Aqueous–Oxide Nanoparticle Interface by XPS from a Liquid Microjet. *Nano Lett.* **2013**, *13*, 5403–5407.
- (7) Mishra, H.; Enami, S.; Nielsen, R. J.; Stewart, L. A.; Hoffmann, M. R.; Goddard, W. A.; Colussi, A. J. Brønsted Basicity of the Air–Water Interface. *Proc. Natl. Acad. Sci. U.S.A.* **2012**, *109*, 18679–18683.
- (8) Pratt, L. R.; Pohorille, A. Hydrophobic Effects and Modeling of Biophysical Aqueous Solution Interfaces. *Chem. Rev.* **2002**, *102*, 2671–2692.
- (9) Chaudhury, M. K.; Whitesides, G. M. How to Make Water Run Uphill. *Science* **1992**, *256*, 1539–1541.
- (10) Ichimura, K.; Oh, S.-K.; Nakagawa, M. Light-Driven Motion of Liquids on a Photoresponsive Surface. *Science* **2000**, *288*, 1624–1626.
- (11) Berna, J.; Leigh, D. A.; Lubomska, M.; Mendoza, S. M.; Pérez, E. M.; Rudolf, P.; Teobaldi, G.; Zerbetto, F. Macroscopic Transport by Synthetic Molecular Machines. *Nat. Mater.* **2005**, *4*, 704–710.
- (12) Quéré, D.; Ajdari, A. Liquid Drops: Surfing the Hot Spot. *Nat. Mater.* **2006**, *5*, 429–430.
- (13) Pamme, N. Magnetism and Microfluidics. *Lab Chip* **2006**, *6*, 24–38.
- (14) Barbulovic-Nad, I.; Xuan, X.; Lee, J. S.; Li, D. DC-Dielectrophoretic Separation of Microparticles Using an Oil Droplet Obstacle. *Lab Chip* **2006**, *6*, 274–279.
- (15) Prins, M. W. J.; Welters, W. J. J.; Weekamp, J. W. Fluid Control in Multichannel Structures by Electrocapillary Pressure. *Science* **2001**, *291*, 277–280.
- (16) Gallardo, B. S.; Gupta, V. K.; Eagerton, F. D.; Jong, L. I.; Craig, V. S.; Shah, R. R.; Abbott, N. L. Electrochemical Principles for Active Control of Liquids on Submillimeter Scales. *Science* **1999**, *283*, 57–60.
- (17) Ban, T.; Yamagami, T.; Nakata, H.; Okano, Y. pH-Dependent Motion of Self-Propelled Droplets Due to Marangoni Effect at Neutral pH. *Langmuir* **2013**, *29*, 2554–2561.
- (18) Sanchez, S.; Ananth, A. N.; Fomin, V. M.; Viehriq, M.; Schmidt, O. G. Superfast Motion of Catalytic Microjet Engines at Physiological Temperature. *J. Am. Chem. Soc.* **2011**, *133*, 14860–14863.
- (19) Zhao, G.; Sanchez, S.; Schmidt, O. G.; Pumera, M. Poisoning of Bubble Propelled Catalytic Micromotors: the Chemical Environment Matters. *Nanoscale* **2013**, *5*, 2909–2914.
- (20) Phan, C. M. Stability of a Floating Water Droplet on an Oil Surface. *Langmuir* **2014**, *30*, 768–773.
- (21) Ristenpart, W. D.; Bird, J. C.; Belmonte, A.; Dollar, F.; Stone, H. A. Non-coalescence of Oppositely Charged Drops. *Nature* **2009**, *461*, 377–380.
- (22) Kurimura, T.; Ichikawa, M.; Takinoue, M.; Yoshikawa, K. Back-and-Forth Micromotion of Aqueous Droplets in a DC Electric Field. *Phys. Rev. E* **2013**, *88*, 042918.
- (23) Nguyen, C. V.; Phan, C. M.; Ang, H. M.; Nakahara, H.; Shibata, O.; Moroi, Y. Surface Potential of 1-Hexanol Solution: Comparison with Methyl Isobutyl Carbinol. *J. Phys. Chem. B* **2013**, *117*, 7615–7620.
- (24) Rane, J. P.; Pauchard, V.; Couzis, A.; Banerjee, S. Interfacial Rheology of Asphaltenes at Oil–Water Interfaces and Interpretation of the Equation of State. *Langmuir* **2013**, *29*, 4750–4759.
- (25) Nordgård, E. L.; Simon, S.; Sjöblom, J. Interfacial Shear Rheology of Calcium Naphthenate at the Oil/Water Interface and the Influence of pH, Calcium, and in Presence of a Model Monoacid. *J. Dispersion Sci. Technol.* **2012**, *33*, 1083–1092.
- (26) Liu, T.; Seiffert, S.; Thiele, J.; Abate, A. R.; Weitz, D. A.; Richtering, W. Non-coalescence of Oppositely Charged Droplets in pH-Sensitive Emulsions. *Proc. Natl. Acad. Sci. U.S.A.* **2012**, *109*, 384–389.
- (27) van den Heuvel, M. G. L.; Dekker, C. Motor Proteins at Work for Nanotechnology. *Science* **2007**, *317*, 333–336.
- (28) Wang, J.; Manesh, K. M. Motion Control at the Nanoscale. *Small* **2010**, *6*, 338–345.
- (29) Zhao, B.; Moore, J. S.; Beebe, D. J. Surface-Directed Liquid Flow Inside Microchannels. *Science* **2001**, *291*, 1023–1026.
- (30) Hao, L.; Su, J.; Guo, H. Water Permeation through a Charged Channel. *J. Phys. Chem. B* **2013**, *117*, 7685–7694.
- (31) Tanyeri, M.; Schroeder, C. M. Manipulation and Confinement of Single Particles Using Fluid Flow. *Nano Lett.* **2013**, *13*, 2357–2364.
- (32) Santoso, S.; Hwang, W.; Hartman, H.; Zhang, S. Self-Assembly of Surfactant-Like Peptides with Variable Glycine Tails to Form Nanotubes and Nanovesicles. *Nano Lett.* **2002**, *2*, 687–691.
- (33) Dexter, A. F.; Malcolm, A. S.; Middelberg, A. P. Reversible Active Switching of the Mechanical Properties of a Peptide Film at a Fluid–Fluid Interface. *Nat. Mater.* **2006**, *5*, 502–506.
- (34) Shchipunov, Y. A.; Schmiedel, P. Phase Behavior of Lecithin at the Oil/Water Interface. *Langmuir* **1996**, *12*, 6443–6445.